Formation and Characterization of Polyamide Composite Electrospun Nanofibrous Membranes for Salt Separation

Satinderpal Kaur,[1] Subramanian Sundarrajan,[1] Renuga Gopal,[1] Seeram Ramakrishna[1,2]

[1]*Nanoscience and Nanotechnology Initiative, Faculty of Engineering, National University of Singapore, Singapore*
[2]*King Saud University, Riyadh 11451, Kingdom of Saudi Arabia*

Received 23 June 2010; accepted 1 October 2011
DOI 10.1002/app.36375
Published online 15 January 2012 in Wiley Online Library (wileyonlinelibrary.com).

ABSTRACT: Currently, electrospun nanofibrous membranes (ENMs) are classified in the microfiltration range. In this study, we explored the applicability of using ENMs for nanofiltration (NF) applications through a surface modification approach. A polyamide layer was formed on the surface of the ENMs through interfacial polymerization with two different approaches. In the first approach (approach A), ENMs were soaked in an aqueous phase followed by an organic phase; in the second approach (approach B), we reversed this sequence. This resulted in different surface morphologies over the ENM surface. The best approach B allowed the separation of 80.7% of 2000-ppm $MgSO_4$ and 67.0% of 2000-ppm NaCl at a pressure of 70 psig under a dead-end filtration setup. The fluxes attained were 0.51 and 0.52 L m^{-2} h^{-1}, respectively. In addition, the effect of the pore size on the formation of a polyamide film was investigated. It was realized that bubble points of 1.8 and 3.4 μm were both able to support the polymer film on its surface, but their separation efficiency differed slightly. These findings suggest that ENMs could be used beyond their current microfiltration stage, and hence, their use could be widened to NF membranes. © 2012 Wiley Periodicals, Inc. J Appl Polym Sci 124: E205–E215, 2012

Key words: composites; membranes; nanofiber; polyamides

INTRODUCTION

Electrospinning[1,2] is a fiber-forming process that uses a high-voltage electric field to produce an electrically charged jet of polymer fluid, which on solidifying, produces a fibrous web composed of fibers from a few nanometers to submicrometer in diameter.[3] Initial research focused on the optimization of the conditions to obtain these fibers in the nanorange. Since then, there has been an upsurge of research focusing on the use of these materials in several applications because of their attractive attributes, including a fiber morphology similar to that of the extracellular matrix,[4,5] a large surface area per unit volume, high porosity due to an interconnected open-pore structure, high permeability for gases,[6,7] and potential for the incorporation of an active chemistry or functionality.[8] This has resulted in electrospun nanofibrous webs being used successfully as scaffolds in tissue engineering[9,10] and has found commercial success in high-performance air filters.[11] However, their use as a liquid filter is at its infancy, and intense research has recently commenced, which might provide a wider platform for liquid separation.

One of the drawbacks of electrospun nanofibers for use in liquid separation is that they are mechanically unstable when compared to cast membranes; that is, they are too weak to withstand pressure during separation. Apart from this, when a membrane is formed, the fiber layers detach easily, and thereby, the overall structure of the membrane is damaged. To use them for separation technology, an additional support layer is generally required to provide strength.

However, Gopal and co-workers[12,13] showed that with heat treatment, electrospun nanofibrous membranes (ENMs) can be used as self-supporting membranes. The separation of different sizes of polystyrene beads on poly(vinylidene fluoride) (PVDF) and polysulfone electrospun membranes were evaluated. They concluded that the ENMs had a symmetrical structure and were able to separate microparticles above their bubble points (the largest pore present) effectively without fouling. Aussawasathien et al.[14] performed a similar study using the hydrophilic polymeric material nylon 6 instead and came to a similar conclusion that had been earlier obtained with hydrophobic-based electrospun polymers.

Correspondence to: S. Kaur (satinpal@gmail.com) or S. Ramakrishna (seeram@nus.edu.sg).

Contract grant sponsors: Environment and Water Industry Development Council (Government of Singapore) through the funded project "Development of Low Pressure, High Flux UF and NF Membranes Based on Electrospun Nanofibers for Water Treatment.", National University of Singapore (NUS) Nanoscience and Nanotechnology Initiative.

In an attempt to further reduce the surface pore size of electrospun membranes and, thereby, to use them beyond their microfiltration range application, Kaur et al.[15] used plasma-induced grafting, which created an asymmetric membrane structure. Various grafting techniques have also been employed to impart specific surface chemistries to the fiber surface for their use as affinity membranes for both biological[16,17] and wastewater treatment[18] applications. Wang et al.[19] coated the surface of an electrospun polyacrylonitrile (PAN) nanofibrous membrane with a layer of chitosan, and this ultrafiltration composite membrane was subsequently used to separate oil from wastewater.

ENMs can be further applied to the nanofiltration (NF) range for the separation of monovalent and multivalent ions applications by the further reduction of their pore sizes. This can be accomplished by the introduction of a thin-film coating over the ENMs. The thin-film coating is usually made by chemical and physical means. The interfacial polymerization technique[20] has been widely used in chemical means over other supports to prepare thin-film composites (TFCs). This TFC material[21] should possess necessary characteristics, including a required hydrophilicity for the water to pass through and desired surface characteristics for less fouling.[22]

In this study, PVDF ENMs were surface-modified with a polyamide layer through interfacial polymerization techniques with two different approaches. To the best of our knowledge, this is the first report on the reduction of the pore size of PVDF ENMs by the interfacial polymerization technique. We also evaluated the approach-dependent behavior on the quality of film formation and demonstrated the separation efficiency of the membrane for monovalent and divalent salts.

EXPERIMENTAL

Materials

Analytical-grade hexane (99%), ethanol, *N*,*N*-dimethyl acetamide, and acetone were purchased from Sigma-Aldrich Missouri (MO). The reagents *p*-phenylenediamine (PPD), trimesoyl chloride (TMC), sodium hydroxide (NaOH), and sodium carbonate (Na_2CO_3) were also purchased from Sigma Aldrich. PVDF Kynar 760 was obtained from Arkema (Singapore). Sodium chloride (NaCl) and calcium chloride ($CaCl_2$) were purchased from Merck (Germany, Hesse), and magnesium sulfate hydrate was purchased from Sino Chemical (China, Guangxi). Insulating tape (DENKA, Vini tape) was manufactured in Japan (Tokyo).

Preparation of ENMs

Two different PVDF concentrations, 9 and 15% (w/v), were prepared in a mixture of *N*,*N*-dimethyl acetamide and acetone at a ratio of 2 : 3.

A syringe pump (#KDS 100, KD Scientific Holliston, Massachusetts (MA), USA), (Fisher Scientific) was used to supply a constant flow of 4 mL/h polymer solution during electrospinning. A voltage of 15 kV (Gamma High Voltage Research, Inc.) was applied to the drawn nanofibers from the prepared solution. The fibers were collected on a grounded 10-cm^2 aluminum plate. After the membranes were formed, they were heated from room temperature to 60°C for 1 h at a rate of 1°C/min. The membranes were then heated up to 157°C at the same rate and were subsequently heated at this temperature for 3 h to improve the structural integrity of the membrane. The membranes developed from the 9% (w/v) PVDF solution are referred to as ENM-A, and those developed from the 15% (w/v) PVDF solution are referred to as ENM-B.

The fiber diameters were determined from the field emission scanning electron microscopy (FE-SEM) image with the ImageJ software (http://rsb.info.nih.gov/ij/). All data were expressed as mean plus or minus the standard deviation. Levels of significance were calculated with Student's t test ($n = 30$). Differences were considered statistically significant at $p \leq 0.05$.

Preparation of the composite ENMs

A polyamide layer was formed through the reaction of PPD and TMC. An aqueous solution containing 1% (w/v) of PPD and an organic solution of 0.25% (w/v) TMC in hexane were prepared. Two approaches were studied. After interfacial polymerization, the membranes were heat-treated at 80°C for 10 min. Subsequently, they were washed with copious amounts of water to remove unreacted reactants and loose film.

Approach A: Immersion in the aqueous phase first

PVDF ENM-A and ENM-B were first taped with an insulating tape onto a glass plate and immersed in 1% (w/v) PPD/water (aqueous phase) for 1, 3, or 5 min. The membranes were subsequently tilted in a vertical position for 5 min, and any excess solution on the surface was removed by gentle dabbing with lint-free paper. Subsequently, these membranes were immediately immersed in a 0.25% (w/v) TMC/hexane (organic phase) solution for 1, 5, or 10 min.

Three additional variations of the interfacial polymerization process discussed previously were carried out. In the first variation, the pretreatment of the ENMs was carried out with 70% (v/v) ethanol, and they were washed several times with water to wet the membranes and were subsequently dipped in a 1% (w/v) PPD/water solution for 3 or 60 min. Thereafter, the membrane was placed in a 0.25% (w/v) TMC/hexane solution for 10 min. In the

second variation, the membrane was exposed to plasma (March Instruments, Massachusetts (MA), USA), at 15 W and 13.56 MHz for 10 s before interfacial polymerization was performed. The third variation involved the preparation of an aqueous PPD solution with 0.1*M* NaOH and a 0.2*M* Na_2CO_3 solution (1 : 1).

Approach B: Immersion in the organic phase first

The reverse of approach A was performed in approach B. Without any taping of the support membranes onto a glass plate, they were soaked in a 0.25% (w/v) TMC/hexane solution for 3 min; this was immediately followed by gentle placement of the membranes on the surface of the PPD/water solution [1% (w/v)]. The concentrations of the organic and aqueous phases were further manipulated (see Table II, shown later). Four different ratios of reactant solutions were prepared, and the ratios within brackets indicate the weight percentages of TMC and PPD: TMC/PPD (1 : 1), TMC/PPD (1 : 2), TMC/PPD (1 : 4) and TMC/PPD (1 : 16). The membrane floated in the aqueous solution, and hence, only one side of the membrane was modified. The contact with the aqueous PPD phase was fixed at 10 min.

Characterization

The surfaces and the cross sections of the membranes were observed by FE-SEM (FEI-QUANTA 200F, The Netherlands). The pore size distribution of the support membrane was evaluated with a capillary flow porometer (Porous Materials, Inc.). Permeation tests were performed on an Amicon stirred cell (model 8010, able to withstand a maximum operating pressure of 75 psig) at operating conditions of 70 psig. The circular composite ENMs, 25 mm in diameter, were stamped out and placed in the test cell with the active layer facing the incoming feed. The effective membrane area was 4.1 cm^2. The membranes were initially pressurized at 70 psig until a constant flux was achieved for at least 3 h consecutively before any salt-separation experiments. This was done to condition the membrane for the pure water permeation and salt separation runs that followed.

An initial feed solution of 2000 ppm was used for each salt separation. For each separation experiment, the first 1 mL of permeate was discarded. The next 2 mL of permeate was collected and analyzed. The percentage of solute rejection was determined with the following equation:

$$\text{Rejection } (\%) = \left(1 - \frac{2\lambda_p}{\lambda_{fo} - \lambda_{fi}}\right) \times 100\%$$

where λ_p is the conductivity of the product ($m\Omega^{-1}$ cm^{-1}), λ_{fo} is the conductivity of the initial feed ($m\Omega^{-1}$ cm^{-1}), and λ_{fi} ($m\Omega^{-1}$ cm^{-1}) is the conductivity of the final feed that was retained in the cell after separation.

The conductivity of the solution was determined with a conductivity meter (Orion 3star, Thermo Scientific, Massachusetts (MA), USA). The separation experiment was repeated three times for each salt. Statistical analysis was carried out, and a value of $p \leq 0.05$ was considered statistically significant.

Static water contact angle measurements were performed on the surfaces of the ENMs with an Advanced Surface Technologies, Inc. VCA2000 video contact angle system (AST products, Billerica, Massachusetts (MA), USA). A thin strip of the membrane material ($\sim 0.7 \times 4$ cm^2) was pasted onto a clean glass slide with double-sided tape. A water drop of 0.5 μL was dispersed onto the membrane surface, and the contact angle was determined with the system software.

The change in the surface chemistry of the ENMs was detected with a multibounce (Germanium crystal) horizontal attenuated total reflection (ATR) Fourier transform infrared spectroscopy (FTIR) instrument (Thermo Nicolet Avatar 360 Waltham, Massachusetts (MA), USA). Each spectrum was obtained by the accumulation of 64 scans at a resolution of 8 cm^{-1}.

RESULTS AND DISCUSSION

Electrospun nanofiber support membranes

When the solution with a 9% (w/v) polymer concentration was electrospun and its morphology inspected under FE-SEM (FEI-QUANTA 200F, The Netherlands, Eindhoven) Capillary flow porometer, CFP-1200-A (Ithaca, NY, USA), the presence of beads along with the fibers was observed [Fig. 1(a)]. The fiber diameter was found to be 249 ± 80 nm. When the concentration of the polymer was increased to 15% (w/v), the formation of bead-free fibers with increased average fiber diameter (353 ± 153 nm) was observed [Fig. 1(b)]. This was because the polymer solution concentration is one of the important factors in determining the fiber size and morphology.[4] The formation of beads and beaded fibers is driven by the surface tension.[23] Generally, at a low polymer concentration, the viscosity of the solution is not sufficient enough to form a stable jet. There is capillary breakup of the electrospinning jet by surface tension, which leads to the formation of beads.[24] As the polymer solution concentration increases, the polymer solution viscosity subsequently increases, and the deformation forces in the solidification process are greatly reduced; this leads to the formation of uniform fibers.[25]

Even though the membrane thickness (ca. 120 μm) was constant for both ENM-A and ENM-B, the difference in the two membrane architectures gave rise

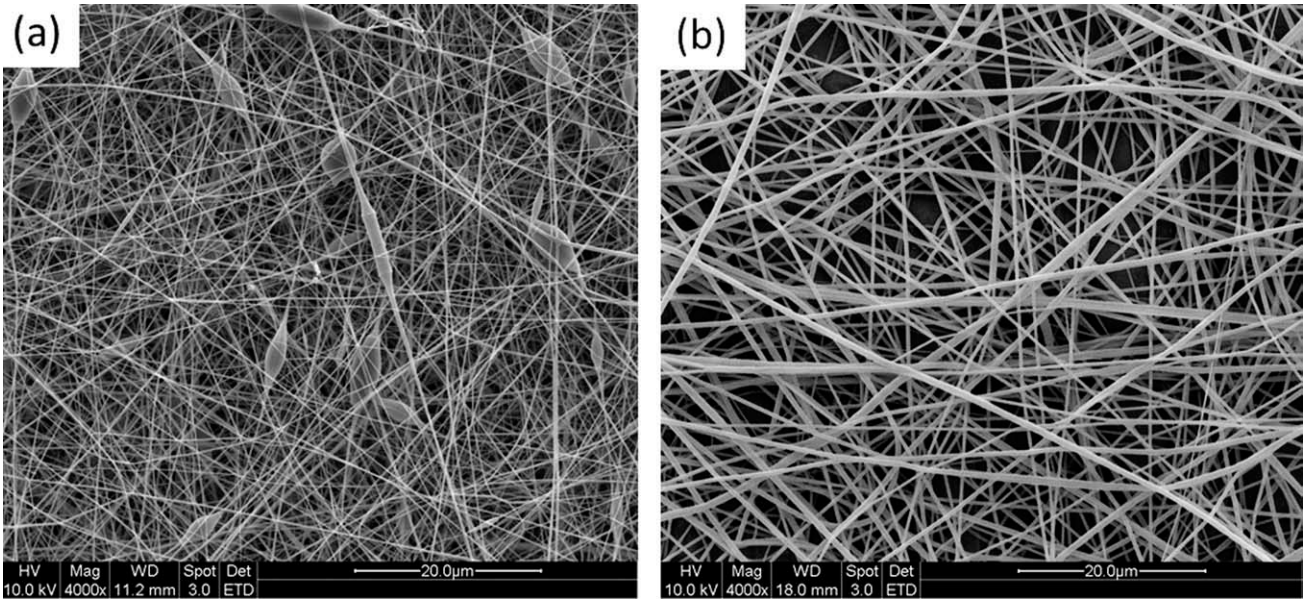

Figure 1 Surface architecture of (a) ENM-A [9% (w/v)] and (b) ENM-B [15% (w/v)].

to different pore size distributions. An overview of the membrane's characteristics is listed in Table I. The difference in the pore size distribution (range = 0.2–1.8 μm, Fig. 2) in ENM-A was attributable to the presence of beads, and finer fiber diameters gave rise to a higher packing density and, hence, smaller pores in ENM-A compared to ENM-B (pore size range = 0.7–3.4 μm, Fig. 3) and smaller fiber diameters.

Composite membrane fabrication: Approach A

Figure 4(a–c) depicts the extent of the thin surface layer formed on the ENMs with approach A, with immersion periods of 3, 60, and 120 min, respectively, in the aqueous PPD solution. As shown in the micrographs, no film was formed after 3 min of immersion [Fig. 4(a)], whereas some film started to be formed between the pores after 60 min of immersion [Fig. 4(b)]. Although some clear thin-film formation occurred after the extended immersion period (for 120 min), film formation was not homogeneous across the ENMs, and the presence of pin holes or defects on the surface were observed, which would be undesirable for subsequent filtration.

This nonuniformity was possibly due to the hydrophobic nature of the ENMs (surface contact angle = 135°), and we postulated that the aqueous PPD solution could not penetrate into the pore of the hydrophobic ENMs. This may have led the PPD to not be retained uniformly on the surface of ENMs, which were reacting with TMC in the organic phase in the second stage. It is noted here that the hydrophobic nature of the ENMs was due to their inherent surface roughness and trapped air pockets; this was already reported in our previous article.[15] Similar results were observed in the case of ENM-A as well, and the scanning electron microscopy (SEM) images are not presented here.

To overcome the problem of the high hydrophobicity of the ENMs and to make them uniformly wettable by aqueous PPD solution, three variations were carried out: (1) prewetting of the ENMs with 70% (v/v) ethanol, (2) preparation of the PPD solution with NaOH and Na_2CO_3, and (3) exposure of the ENM to plasma.

Enhancement in the wettability by the aqueous ethanol treatment

In the first variation, the PVDF ENM was prewetted with a 70% (v/v) aqueous ethanol solution; this was followed by interfacial polymerization, which led to

TABLE I
Summary of the Membrane Characteristics

Membrane	PVDF solution % (w/v)	Fiber diameter (nm)	Largest pore (μm)	Smallest pore (μm)	Membrane thickness (μm)
ENM-A	9	249 ± 80	1.8	0.2	~ 120
ENM-B	15	353 ± 153	3.4	0.7	~ 120

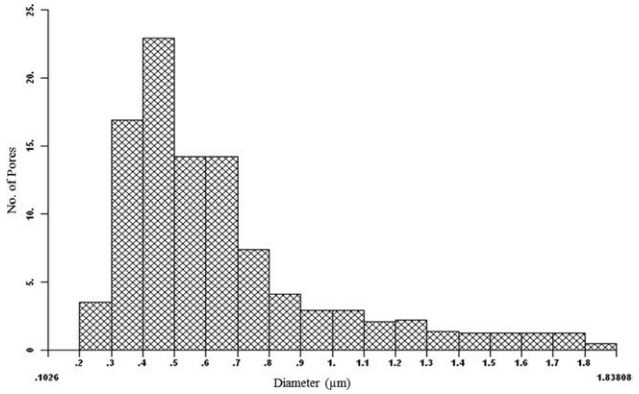

Figure 2 Pore size distribution of the support ENM-A electrospun from 9% (w/v) PVDF solution.

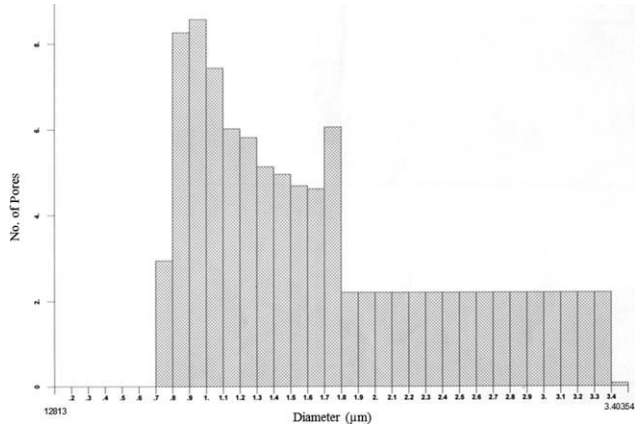

Figure 3 Pore size distribution of the support ENM-B electrospun from 15% (w/v) PVDF solution.

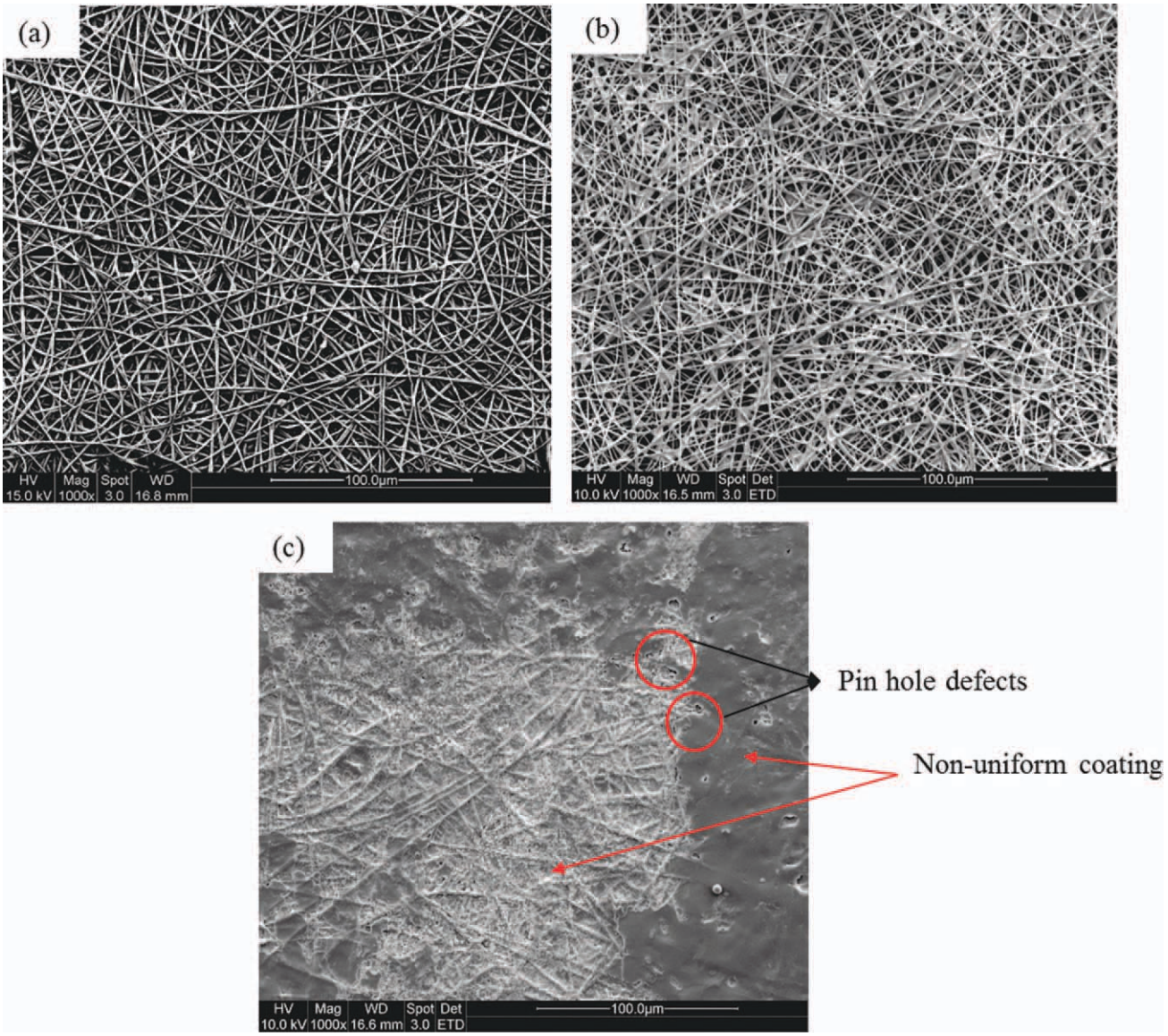

Figure 4 Approach A: Surface architecture of ENMs-B after they were immersed in the aqueous phase for (a) 3, (b) 60, and (c) 120 min followed by 10 min of soaking in the organic phase. [Color figure can be viewed in the online issue, which is available at wileyonlinelibrary.com.]

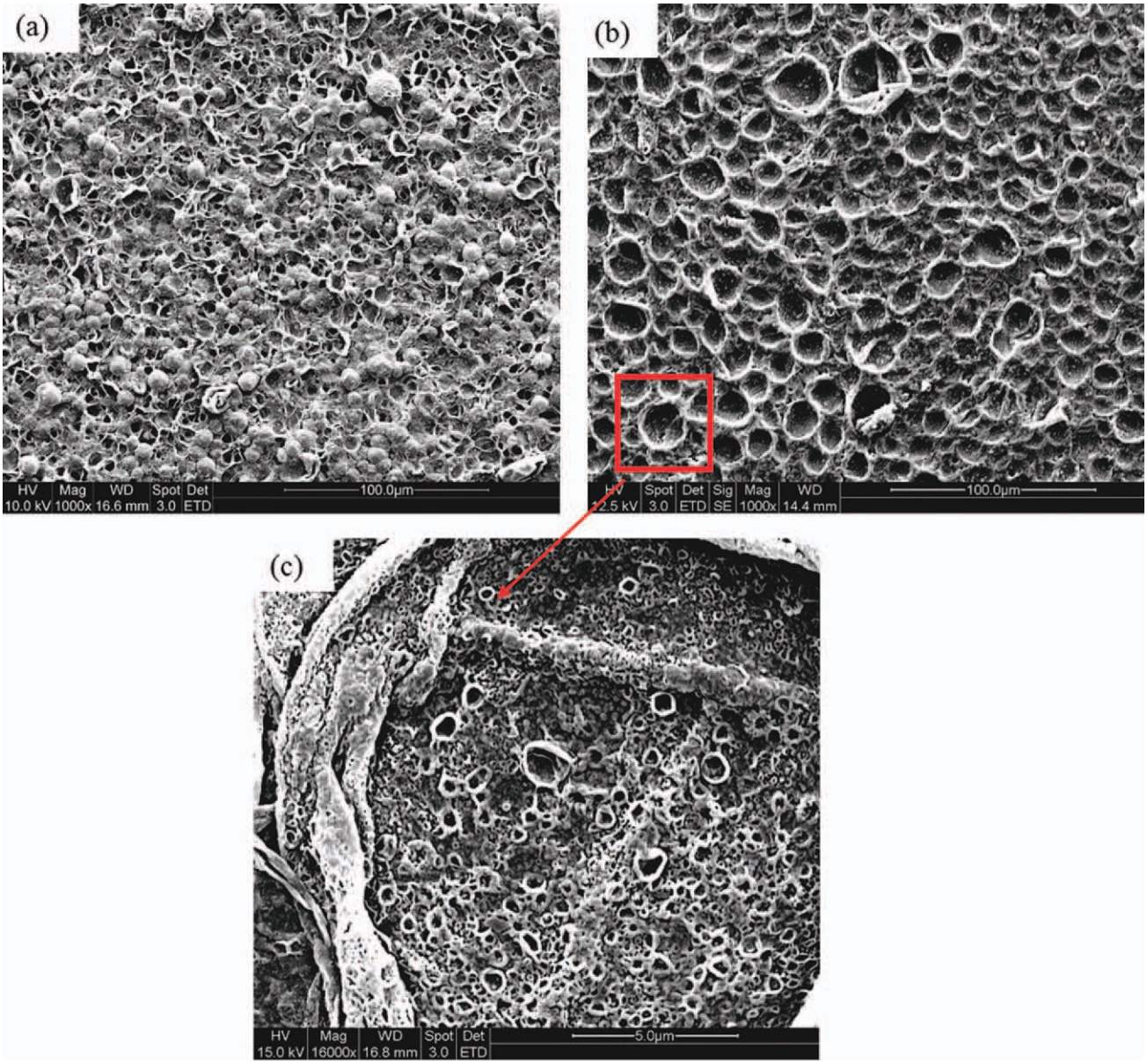

Figure 5 Surface architectures of ENMs-B after they were wetted with aqueous ethanol first followed by immersion in the aqueous phase (approach A) for (a) 3 and (b) 60 min and subsequent soaking in organic phase for 10 min. (c) Higher magnification of part (b). [Color figure can be viewed in the online issue, which is available at wileyonlinelibrary.com.]

the formation of a deep purple film on the surface of the ENM. When the membrane was prewetted with ethanol, the contact angle of the membrane was reduced from 135 to 0°. When the PVDF ENM was soaked in the PPD phase for 3 min followed by a 10-min reaction with the TMC phase, a coarse and rough surface with globulelike structures was observed with the formation of the polyamide film [Fig. 5(a)]. When the immersion time was increased from 3 to 60 min, the film adopted a honeycomb structure [Fig. 5(b)]. This could have been due to the formed globulelike structure for the lower immersion time burst to give the honeycomb appearance and/or directing capability of more available PPD molecules at a higher immersion time for the reaction with TMC.

Although the film was formed on the ENM surface, these membranes were not able to reject any salt. A closer inspection of the honeycomb structure [Fig. 5(c)] indicated that many holes were observed on the surface, which most probably resulted in the unsuccessful rejection of salts.

Immersion in a basic solution

The PPD solution was prepared with NaOH and Na_2CO_3 solutions to wet the membrane easily. Also, they were added as acid receptors to neutralize the

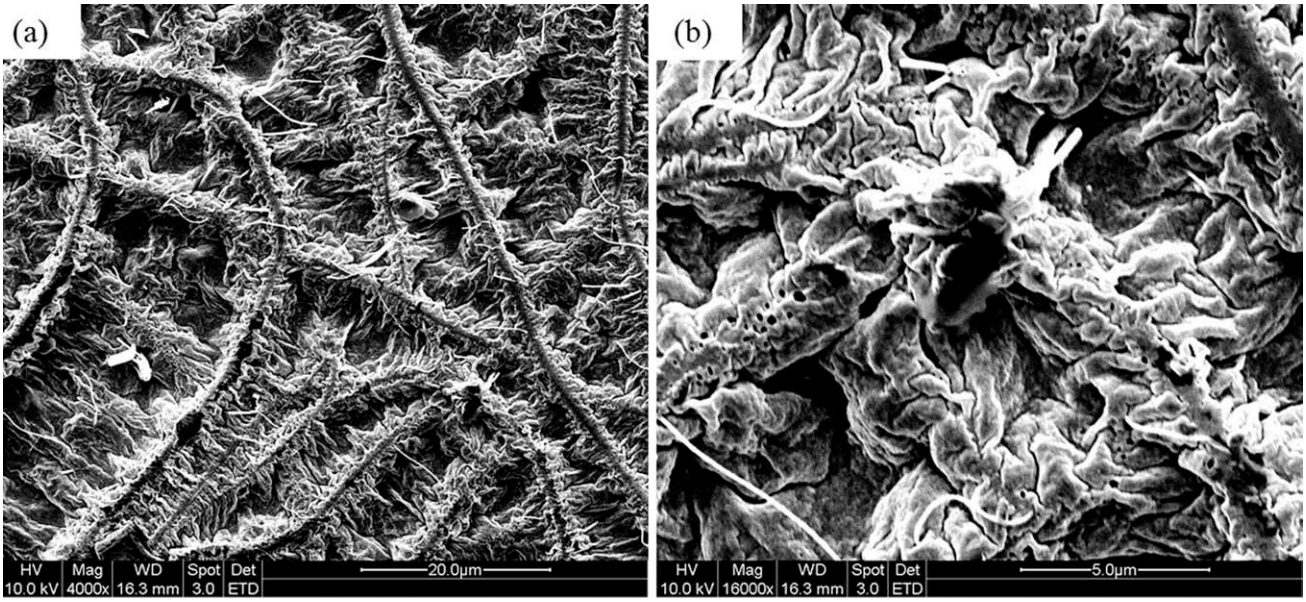

Figure 6 Surface architecture of the film formed on the surface of ENM-B when the aqueous PPD solution was prepared with a 0.1*M* NaOH solution and 0.2*M* Na_2CO_3: (a) 4000 and (b) 160,000×.

hydrogen chloride generated during the formation of the polyamide via reaction of the acid halide and the amine solution.[26]

The film formed on the surface of the support ENM is shown in Figure 6 and looked completely different when the membrane was prewetted with 70% (v/v) ethanol instead. The added additives played an important role in the way the film was formed and also tended to influence the monomer solubility, diffusivity, hydrolysis, and protonation and to scavenge inhibitory reaction byproducts. It was reported in the literature that any factors that alter the solubility and diffusivity of the amine monomer in the organic phase affect the reaction rate and, thus, the morphology and structure of the resulting polyamide film.[27] Although the membranes morphologies were different, they did not influence the separation tendency, and they were also not able to separate any monovalent and divalent salts. The magnification of the surface under SEM [Fig. 6(b)] clearly indicated that there were many holes on the film, and this may have prevented the separation of salts.

Plasma treatment

When the support ENM was exposed to plasma, the membrane surfaces were easily wetted by the aqueous phase. However, there was no film formed on the surface of the membrane. Plasma exposure prevented any film formation on the surface of the membrane, and this is reflected in Figure 7.

Composite membrane fabrication: Approach B

Using approach B, composite polyamide films on both ENM-A and ENM-B without any defects were successfully made. The surface topography of the composite ENMs is shown in Figure 8. One advantage of this approach was that interfacial polymerization could be carried out without the fixing of the membrane on a glass plate; hence, this saved time. We believe this approach is generally not preferred for conventional phase-inverted membranes as the membranes are coagulated in a water bath and stored in water. It was obvious that the application of approach B required the drying of the support. It added another step to membrane preparation; hence,

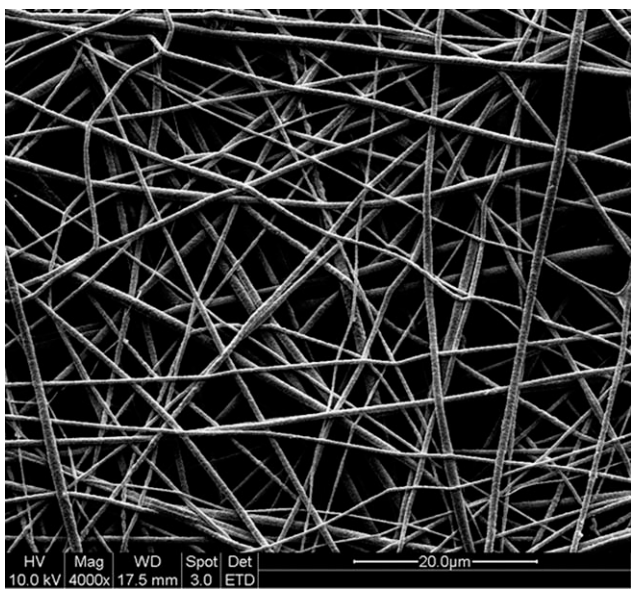

Figure 7 Surface morphology of ENM-B after exposure to plasma and subsequently to interfacial polymerization with approach A.

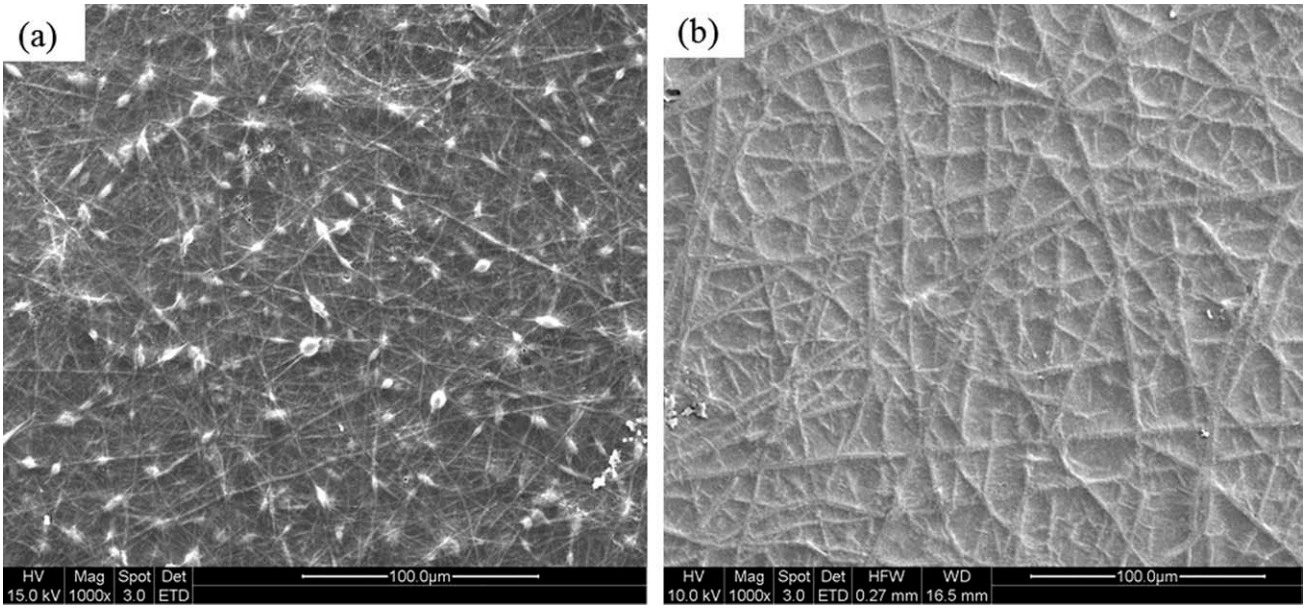

Figure 8 Polyamide films on the surfaces of (a) ENM-A and (b) ENM-B.

approach A would generally be used for conventional phase-inverted membranes. However, in this instance, PVDF was hydrophobic, and hence, it was more suitable for immsering the membranes in an organic phase first followed by interfacial polymerization.

The separation of $MgSO_4$ was carried out on both composites ENM-A and ENM-B. When 2000-ppm $MgSO_4$ was used as a feed solution, composite ENM-A was able to achieve a salt rejection of 70.2% at a flux of 0.62 L m^{-2} h^{-1}, whereas composite ENM-B achieved a salt rejection of 75.3% at a flux of 0.66 L m^{-2} h^{-1}. Composite ENM-B showed better separation efficiency in terms of flux and rejection, which could be explained as follows. First, ENM-B had a larger bubble point than ENM-A and, hence, had a higher flux than ENM-A. Second, ENM-A had beaded fibers, which might have affected the packing nature of the polymer chain in the polyamide film. This could have subsequently reduced the percentage rejection of $MgSO_4$ in ENM-A.

The results obtained for the separation of various salts for ENM-B are shown in Figure 9. A NaCl rejection of 61.6% at a flux of 0.56 L m^{-2} h^{-1} was obtained for 2000-ppm NaCl. In addition, the rejection of 2000-ppm $CaCl_2$ was 70.2%, and the flux attained was 0.77 L m^{-2} h^{-1}. The rejection and flux of $MgSO_4$ was significantly higher than those of NaCl and $CaCl_2$ ($p \leq 0.05$). The observed order of solute rejection for various salts was NaCl < $CaCl_2$ < $MgSO_4$. This could be explained as follows. The hydration numbers (or related measures of hydrated ion size) measured for the sodium, calcium, and magnesium ions in water were 1.66, 5.29, and 7.06, respectively,[28] and hence, greater amounts of magnesium sulfate were rejected versus NaCl. Apart from this, when we compared the hydrated radii of anions between chloride and sulfate ions, the hydrated radii of chlorine and sulfate were 0.19 and 0.30 nm, respectively.[29]

Because a successful film was formed with 0.25% (w/v) TMC and 1% (w/v) PPD, the ratio of the monomers were varied to study the effect on film formation and separation. The resulting concentrations studied are reflected in Table II. The rejection and separation profile of the composite ENM that was formed from different TMC and PPD concentration ratios is shown in Table III.

The surface architecture of the modified membrane when the concentration of both PPD and TMC

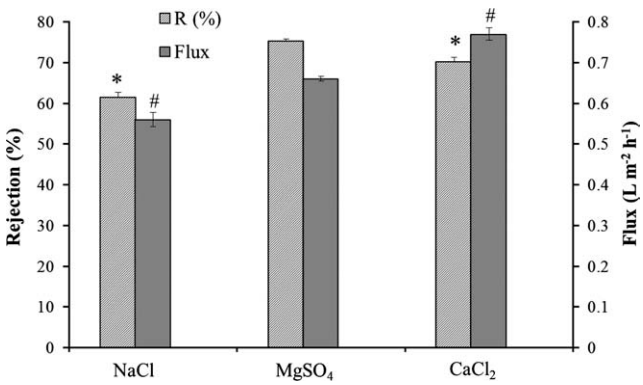

Figure 9 Performance of the membranes prepared by approach B, where the support ENM-B was soaked in 0.25% (w/v) TMC solution in hexane for 3 min and then one surface contacted with 1% (w/v) aqueous PPD solution for 10 min. An asterisk (*) indicates significance against $MgSO_4$ rejection at $p \leq 0.05$, and a number sign (#) indicates significance against $MgSO_4$ flux at $p \leq 0.05$.

TABLE II
Effect of Concentration on the Formation of Interfacial Polymerization

Approach B	Ratio of TMC concentration to PPD concentration	TMC concentration (% w/v)[a]	PPD concentration (% w/v)[b]
i	1 : 1	1	1
ii	1 : 2	0.5	1
iii	1 : 4	0.25	1
iv	1 : 16	0.25	4

[a] TMC immersion time, 3 min.
[b] PPD immersion time, 10 min.

solution was 1% (w/v), is shown in Figure 10. The salt rejection was 0%; this was due to the incomplete formation of the thin film on the surface of the membrane. When the ratio was 1 : 2; that is, the TMC concentration was 0.5% (w/v) and the PPD concentration was 1% (w/v), the $MgSO_4$ and NaCl rejections were 42.0 and 42.5%, respectively. The ratio of TMC to PPD was modified to 1 : 16 to ensure that there was excess PPD to react completely with TMC to form a better crosslinked film. When the ratio was changed to 1 : 16 with the same soaking times of 3 min in TMC and 10 min in PPD, an $MgSO_4$ rejection of 80.7% with a flux of 0.51 L m^{-2} h^{-1} and an NaCl rejection of 67.0% with a flux of 0.52 L m^{-2} h^{-1} were achieved. By increasing the concentration of PPD with respect to the concentration of TMC, better separation results were achieved. This was because of the trifunctional nature (which was 3) of the TMC molecule, which was more than that in the PPD molecule. Stoichiometrically, a larger number of PPD was necessary to complete the crosslinking of polyamide chains, and/or the higher concentration may have prevented the hydrolysis of TMC by a competing reaction and, thereby, favored the formation of polymers. Also, when the concentration of the reactant (PPD) used was low, it may not have been adequate to cover such relatively big

TABLE III
Flux and Separation Profile of the ENM-Based Composite Membranes Made from Different Ratios of Monomer Concentrations

	$MgSO_4$ experiment[a]		NaCl experiment[a]	
Approach B	Rejection (%)	Flux (L m^{-2} h^{-1})	Rejection (%)	Flux (L m^{-2} h^{-1})
i	0	—	0	—
ii	42.0	1.24	42.5	1.20
iii	75.3	0.66	61.6	0.56
iv	80.7	0.51	67.0	0.52

[a] Solute concentration in feed, 2000 ppm; operating pressure, 70 psig.

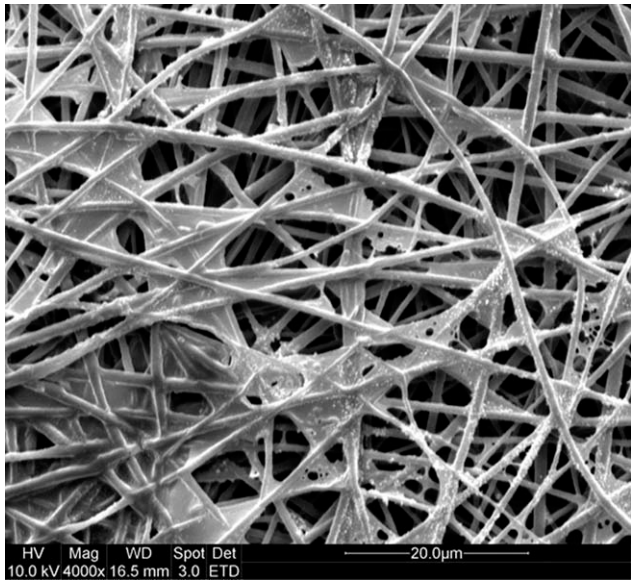

Figure 10 Top surface image of composite ENM-B prepared by approach B(i).

pores present in the ENMs. However, at higher concentrations of the reactant, the possibility of covering the pores by a thin film of polymer may have been high. Hence, the separation was relatively good for the membrane with a high concentration of reactant than for a lower concentration one. It is noted that generally, a higher solution concentration of reactants favors the formation of polymers over the oligomer formation.[30] The cross section of the membrane that was modified with TMC and PPD in the ratio of 1 : 16 is shown in Figure 11. The polyamide layer was uniform throughout the cross section of the membrane and had an approximate thickness of 27 μm. This layer occupied approximately 20% of the entire ENM.

The surfaces of the PVDF ENM, composite ENM B, PPD, and TMC were characterized by ATR–FTIR spectroscopy (Fig. 12). The chemical species present in the polyamide layer were differentiated from the nonmodified PVDF ENM. The spectrum of the composite ENM indicated that interfacial polymerization occurred because the acid chloride band at 1760 cm^{-1} (present in TMC) was absent, and an amide I band at 1650 cm^{-1} (amide I) was present, which was the characteristic —C=O— band of an amide group. In addition to this, another band characteristics of the polyamide layer (amide II, —C—N— stretching) was also seen at 1520 cm^{-1}.

CONCLUSIONS

Interfacial polymerization was carried out on the surface of PVDF ENM by two approaches. These two approaches led to different surface architectures and subsequently different salt rejection values. In

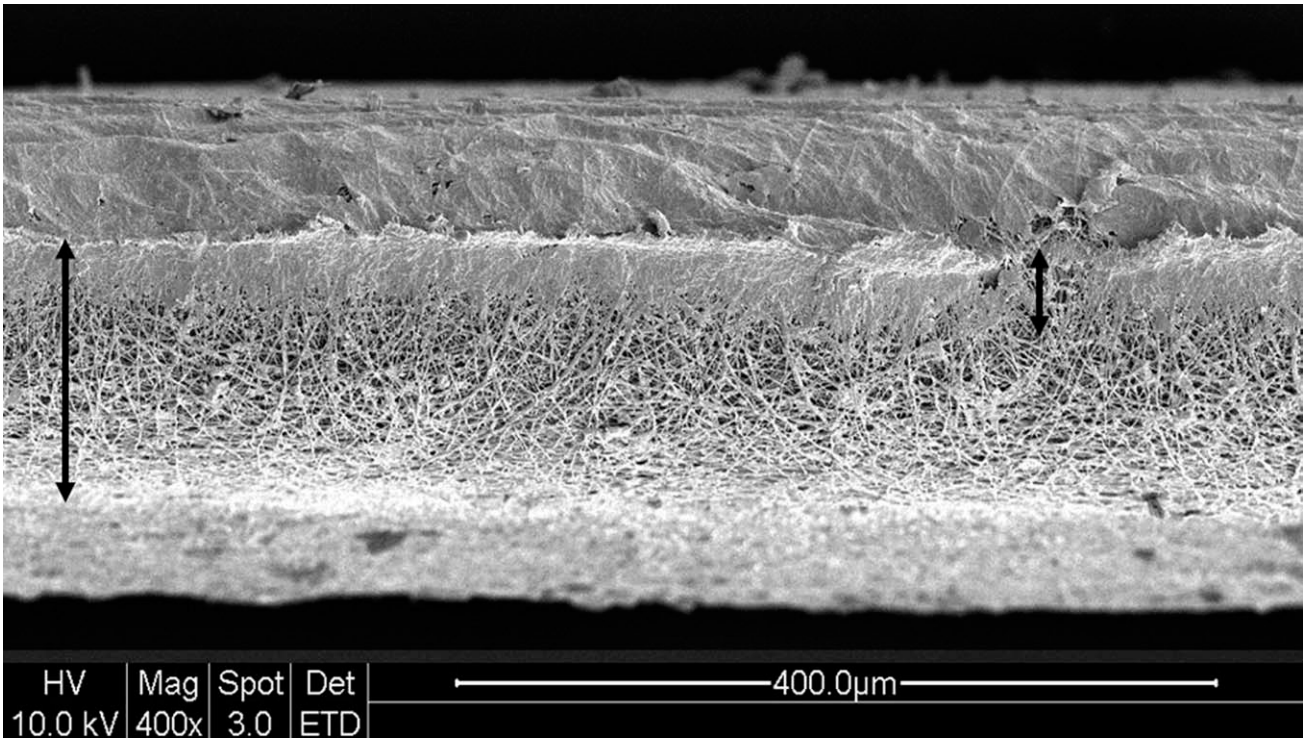

Figure 11 Cross-sectional image of composite ENM-B prepared by approach B(iv).

the first approach (approach A), PVDF–ENM was soaked in an aqueous phase and then in an organic phase. The polyamide film formed was nonuniform because of hydrophobic nature of PVDF–ENM, and thereby, the wettability was poor, and the rejection of salts was not successful. Attempts were made to

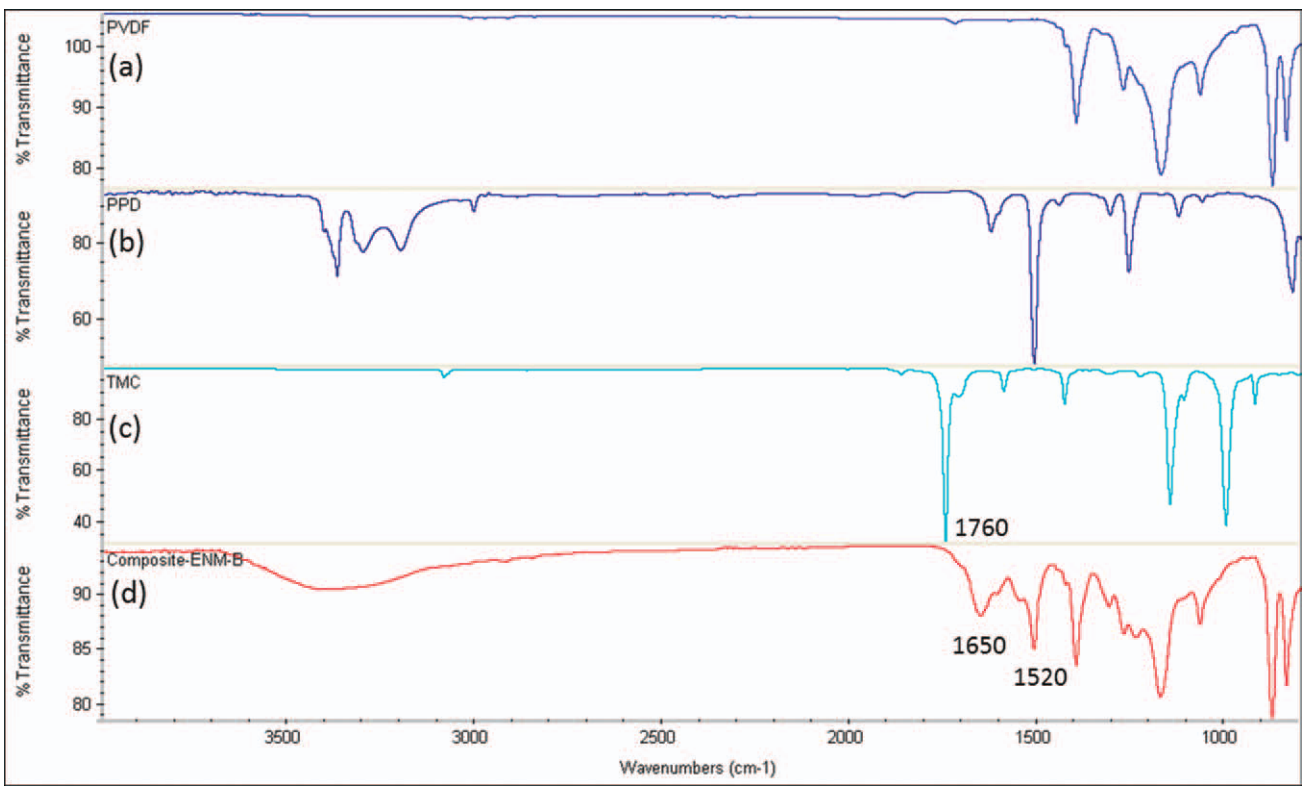

Figure 12 ATR–FTIR spectrum of (a) PVDF ENM, (b) PPD, (c) TMC, and (d) composite ENM-B. [Color figure can be viewed in the online issue, which is available at wileyonlinelibrary.com.]

overcome this hydrophobic nature by chemical and plasma methods. Although interesting architectures were obtained, the rejection of salts remained unsuccessful; this was due to the presence of several tiny holes. The approach B, which included the soaking of PVDF ENM in an organic phase first and then in an aqueous phase, led to the formation of a uniform polyamide film with a wettable surface. This composite membrane was able to reject several salts.

With this approach, composite PVDF–ENMs (ENM-A and ENM-B) with two different pore sizes were prepared. A higher flux and higher salt rejection efficiency were obtained with a membrane of having a larger bubble point and a fine fiber diameter, whereas a comparatively lower flux and lower rejection were obtained with a membrane having beaded fibers.

In addition, it was observed that the difference in the ratio of the monomers during interfacial polymerization played an important role in the overall membrane separation efficiency. When the difference between the two monomers ratio was increased, the rejection of the salts was also increased because of the requirement of a greater concentration of PPD for the polymerization. The best interfacial polymerization conditions performed on the surface of the ENM resulted in the rejection of 80.7% of $MgSO_4$ and 67.0% of NaCl.

The preliminary results produced here highlight the potential of ENMs as self-supporting nanofilters. With careful optimization of the surface film, the rejection rate and flux may be greatly improved. With better optimization and understanding of their separation behavior, efficient nanofilters based on electrospun membranes can be designed and developed.

The authors thank Takeshi Matsuura from the Natural Sciences and Engineering Research Council of Canada for his constant advice on TFC membranes.

References

1. Cooley, J. F. U.S. Pat. 692,631 (1902).
2. Formhals, A. U.S. Pat. 1,975,504 (1934).
3. Huang, Z.; Zhang, Y.; Kotaki, M.; Ramakrishna, S. Compos Sci Technol 2003, 63, 2223.
4. Ramakrishna, S.; Fujihara, K.; Teo, W. E.; Lim, T. C.; Ma, Z. An Introduction to Electrospinning and Nanofibers; World Scientific Publishing: Singapore, 2005.
5. Teo, W. E.; He, W.; Ramakrishna, S. Biotechnol J 2006, 19, 918.
6. Grafe, T.; Graham, K. Nonwoven Technol Rev INJ 2003 (Spring), 51.
7. Barhate, R. S.; Loong, C. K.; Ramakrishna, S. J Membr Sci 2006, 283, 209.
8. Ma, Z.; Kotaki, M.; Ramakrishna, S. J Membr Sci 2006, 272, 179.
9. Shin, M.; Ishii, O.; Sueda, T.; Vacanti, J. Biomaterials 2004, 25, 3717.
10. Prabhakaran, M. P.; Venugopal, J.; Chyan, T. T.; Hai, L. B.; Chan, C. K.; Tang, A. L. Y.; Ramakrishna, S. Tissue Eng 2008, 14, 1787.
11. Barhate, R. S.; Sundarajan, S.; Pliszka, D.; Ramakrishna, S. Filtr Sep 2008, 45(4), 32.
12. Gopal, R.; Kaur, S.; Ma, Z.; Chan, C.; Ramakrishna, S.; Matsuura, T. J Membr Sci 2006, 281, 581.
13. Gopal, R.; Kaur, S.; Feng, C.; Chan, C.; Ramakrishna, S.; Tabe, S.; Matsuura, T. J Membr Sci 2007, 289, 210.
14. Aussawasathien, D.; Teerawattananon, C.; Vongachariya, A. J Membr Sci 2008, 315, 11.
15. Kaur, S.; Zuwei, M.; Gopal, R.; Singh, G.; Ramakrishna, S.; Matsuura, T. Langmuir 2007, 23, 13085.
16. Ma, Z.; Kotaki, M.; Ramakrishna, S. J Membr Sci 2005, 265, 115.
17. Chan, C. K.; Liao, S.; Li, B.; Laureu, R. R.; Larrick, J. W.; Ramakrishna, S.; Raghunath, M. Biomed Mater 2009, 4, 35006.
18. Kaur, S.; Kotaki, M.; Ma, Z. W.; Gopal, R.; Ramakrishna, S. Int J Nanosci 2006, 5, 1.
19. Wang, X.; Fang, D.; Yoon, K.; Hsiao, B. S.; Chu, B. J Membr Sci 2006, 278, 261.
20. Petersen, R. J. J Membr Sci 1993, 83, 81.
21. Larson, R. E.; Cadotte, J. E.; Petersen, R. J. Desalination 1981, 38, 473.
22. Chu, B.; Hsiao, B. S. J Polym Sci Part B: Polym Phys 2009, 47, 2431.
23. Magarvey, R. H.; Outhouse, L. E. J. Fluid Mech 1962, 13, 151.
24. Fong, H.; Chun, I.; Reneker, D. H. Polymer 1999, 40, 4585.
25. Xinhua, Z.; Kwangsok, K.; Dufei, F.; Shaofeng, R.; Benjamin, S. H.; Benjamin, C. Polymer 2002, 43, 4403.
26. Zupancic, J. J.; Raymond, J. U.S. Pat. 4661254 (1987).
27. Ghosh, A. K.; Jeong, B. H.; Huang, X.; Hoek, E. M. V. J Membr Sci 2008, 311, 34.
28. David, F.; Vokhmin, V.; Ionova, G. J Mol Liq 2001, 90, 45.
29. Kiriukhin, M. Y.; Collins, K. D. Biophys Chem 2002, 99, 155.
30. Sundarrajan, S.; Srinivasan, K. S. V. Macromol Rapid Commun 2004, 25, 1406.